AD-A061 454 CALIFORNIA UNIV SAN DIEGO LA JOLLA DEPT OF APPLIED P--ETC F/G 3/2
THE LATITUDINAL STRUCTURE OF SOLAR WIND STREAMS FROM RADIO SCIN--ETC(U)
JUN 78 J J KAUFMAN F19628-77-C-0161
UNCLASSIFIED SCIENTIFIC-1 AFGL-TR-78-0169 NL

| OF |
AD
A061454

END
DATE
FILMED
2-79
DDC

LEVEL II

AFGL-TR-78-0169

12 B.S.

AD A061454

THE LATITUDINAL STRUCTURE OF SOLAR WIND STREAMS FROM RADIO SCINTILLATION OBSERVATIONS

J.J. Kaufman

Dept. of Applied Physics and Information Science
University of California, San Diego
La Jolla, California 92093

Scientific Report No. 1

2 June 1978

Approved for public release; distribution unlimited

AIR FORCE GEOPHYSICS LABORATORY
AIR FORCE SYSTEMS COMMAND
UNITED STATES AIR FORCE
HANSCOM AFB, MASSACHUSETTS 01731

Unclassified

SECURITY CLASSIFICATION OF THIS PAGE (When Data Entered)

REPORT DOCUMENTATION PAGE

READ INSTRUCTIONS BEFORE COMPLETING FORM

1. REPORT NUMBER: AFGL-TR-78-Ø169
2. GOVT ACCESSION NO.
3. RECIPIENT'S CATALOG NUMBER
4. TITLE (and Subtitle): THE LATITUDINAL STRUCTURE OF SOLAR WIND STREAMS FROM RADIO SCINTILLATION OBSERVATIONS
5. TYPE OF REPORT & PERIOD COVERED: Scientific Report No. 1
6. PERFORMING ORG. REPORT NUMBER
7. AUTHOR(s): J.J. Kaufman
8. CONTRACT OR GRANT NUMBER(s): F19628-77-C-Ø161
9. PERFORMING ORGANIZATION NAME AND ADDRESS: Dept of Applied Physics and Information Science, University of California, San Diego, La Jolla, CA 92093
10. PROGRAM ELEMENT, PROJECT, TASK AREA & WORK UNIT NUMBERS: 61102F, 2311G3AD
11. CONTROLLING OFFICE NAME AND ADDRESS: Air Force Geophysics Laboratory, Hanscom AFB, Massachusetts 01731, Monitor/Richard C. Altrock/PHS
12. REPORT DATE: 2 June 1978
13. NUMBER OF PAGES: 17
14. MONITORING AGENCY NAME & ADDRESS (if different from Controlling Office)
15. SECURITY CLASS. (of this report): Unclassified
15a. DECLASSIFICATION/DOWNGRADING SCHEDULE
16. DISTRIBUTION STATEMENT (of this Report): Approved for public release; distribution unlimited
17. DISTRIBUTION STATEMENT (of the abstract entered in Block 20, if different from Report)
18. SUPPLEMENTARY NOTES
19. KEY WORDS (Continue on reverse side if necessary and identify by block number): solar corona, solar wind streams, interplanetary medium, interplanetary scintillations (IPS)
20. ABSTRACT (Continue on reverse side if necessary and identify by block number)

We investigate the relation between the solar corona and high-speed solar wind measured from interplanetary scintillations (IPS). Preliminary results show that regions of high coronal intensity of the 5303 Å Fe XIV green line are associated with low IPS velocities, whereas regions of low intensity are associated with both low and high velocities. There is some indication at high heliographic latitudes that the IPS velocity is inversely correlated with the angular divergence of the coronal magnetic field. We present a new model for the turbulence profile in a solar wind stream, which will be used to refine our

DD FORM 1 JAN 73 1473 EDITION OF 1 NOV 65 IS OBSOLETE

Unclassified

78 11 20 061

405 248

SECURITY CLASSIFICATION OF THIS PAGE(When Data Entered)

20. interpretation of IPS data.

SECURITY CLASSIFICATION OF THIS PAGE(When Data Entered)

Summary

The purpose of this research is to study the latitudinal structure of the solar wind using velocities derived from observations of interplanetary scintillations (IPS) and to compare this structure with measurements of the coronal 5303 Å Fe XIV green line, the white light corona, and the structure of the magnetic field in the lower corona. Preliminary results show that regions of high coronal green line intensity are associated with low IPS velocities, whereas regions of low intensity are associated with both low and high velocities. This suggests an inverse correlation, but the effect is obscured because both data sets are line-of-sight integrals. To eliminate the effects of spatial averaging, we are developing a method for inverting the IPS data to infer the underlying spatial structure of velocity. This work has resulted in a new model for the turbulence profile in a solar wind stream. There is some indication at high latitudes that the IPS velocity is inversely correlated with the angular divergence of the coronal magnetic field.

Introduction

It is well known that high-speed solar wind streams measured by spacecraft are associated with coronal regions of low X-ray emission, known as coronal holes (Krieger, Timothy, and Roelof, 1973). Such streams cause geomagnetic disturbances which often recur at 27-day intervals (Snyder, Neugebauer, and Rao, 1963). Coronal holes can also be identified from coronal observations of Fe XIV 5303 Å (Fisher and Musman, 1975), white light, EUV, and He 10830 Å (c.f. Sime, 1976, and references cited therein).

High latitude solar wind velocities can be estimated from observations of IPS (Dennison and Hewish, 1967). It has been shown that high IPS velocities are well correlated with coronal holes as determined in X-ray, EUV, and white light (Rickett, Sime, Sheeley, Crockett, and Tousey, 1976; Sime, 1976). There are indications that high spacecraft velocities are associated with coronal regions where the magnetic field diverges least (Levine, Altschuler, and Harvey, 1977).

In this report we describe an ongoing study to determine the latitudinal structure of the solar wind from IPS observations of 1972-1978 made at the UCSD solar wind observatory. The interpretation of IPS measurements in terms of the underlying solar wind turbulence and velocity structure is discussed. Preliminary results of comparisons between 1) 5303 Å intensities and IPS velocities and 2) coronal magnetic field structure and IPS velocities are given.

Analysis of IPS Data

The UCSD solar wind observatory is a system of three phased arrays separated by distances of about 100 Km and operating at 74 MHz. Radiation from a small angular diameter source is scattered by electron density irregularities in the interplanetary medium, forming a diffraction pattern which drifts over the antenna system at a velocity characteristic of the medium. This velocity is obtained by cross-correlating the signals at the three points of observation.

The UCSD system has operated continuously since 1972, with daily observations of eight radio sources which sample the solar wind at heliographic latitudes of 60°S to 80°N. The IPS velocity, which is the velocity of the drifting scintillation pattern, is obtained by a least squares estimator applied to the time offsets of the cross-correlation functions of intensity from each pair of stations (Kaufman, 1976). Two time offsets are used -- the offset of the peak of the correlation function, giving the "peak" velocity, and the offset of the midpoint of the correlation function at 50% of maximum, giving the "midpoint" velocity. It has been argued that the midpoint velocity is the better estimator of the average solar wind velocity, while the difference between the peak and midpoint velocities gives a rough measure of the range of velocities along the line of sight (Coles and Kaufman, 1978). It has been shown that, because of elongated source structure and elongated density irregularities, the diffraction pattern must be treated as anisotropic when estimating the velocity (Coles and Kaufman, 1978).

We have recently completed an extensive reanalysis of our entire data set, applying second order corrections for filtering errors and standardizing our editing procedure. The most striking general characteristics of the data set are the recurrence of high velocity streams at 27-day intervals, especially during the declining phase of the last solar cycle, and the increase of the average velocity with latitude at a mean rate of 2 Km/sec/degree (Coles, Rickett, and Rumsey, 1974; Coles and Rickett, 1976).

For comparison with coronal data, the IPS velocities must be mapped to the sun. The geometry of an IPS observation is shown in Figure 1. The simplest assumption is that the measured velocity is characteristic of the solar wind at the point of closest approach (PCA) to the sun of the line of sight, where the scattering function is assumed to be maximum. The velocity is mapped from the PCA to a corresponding "sub-scattering" point on the solar surface along the Archimedes spiral given by

$$\Delta\theta = \frac{\omega r}{V} \quad ,$$

where $\Delta\theta$ is the rotation angle of the spiral, r the distance from the sun to the scattering region, ω the sun's angular velocity, and V the measured IPS velocity. The heliographic latitude of the sub-scattering point is determined by the source's ecliptic latitude and its line-of-sight proximity to the sun. The most obvious drawback to this mapping procedure is that the IPS data reflects a line-of-sight integral, and the scattering function is, of course, not a delta function at the PCA. Nevertheless, this procedure gives mappings that are certainly accurate to first order, and it is used in the preliminary results discussed in this report.

Comparison of IPS Velocities with Coronal Observations

Measurements of the corona in Fe XIV 5303 Å (the iron "green line") have been provided by R. Altrock of Sacramento Peak Observatory. The data consist of measurements of the green line intensity at 3° intervals around the solar disc, at heights of 1.15, 1.35, and, for the earlier data, 1.55 solar radii. Observations are typically taken daily, weather permitting, so that the entire corona is mapped in 27 days. A technique for inverting the data to give volume emissivities has been developed at Sac Peak, and emissivity models are available for rotations during which nearly continuous observations were obtained (Fisher and Musman, 1975; Musman and Altrock, 1978). The data currently being studied at UCSD consists of raw intensities from the periods mid-1973 to early 1974 (solar rotations 1600-1611) and fall 1975 to late 1976 (rotations 1631-1649). The former data set covers the Skylab period.

These data have been processed to produce maps of green line intensities for comparison with the IPS velocities. Because of data gaps and the limited latitude coverage of the IPS data during a single rotation, rotation-by-rotation comparisons of the two data sets are of little value. During periods of coronal stability, however, data from several rotations can be averaged together, giving a more complete picture. The most striking feature of these time-average pictures is that the high velocity streams are almost always associated with regions of low green line intensity. The reverse relation, however, is not so clear. This is illustrated in Figure 2, which gives a scatter plot of velocity versus the green line intensity at the inferred stream origin for rotations 1630-1640. Figure 2 shows clearly that high intensity regions are associated with low or average velocities and that high velocities are associated with low intensity regions, but note that many low velocity streams seem to originate from regions of low intensity as well. Thus there is a sort of inverse correlation, as expected, but the relation is clearly not one-to-one. This result may be obscured by temporal evolution of the corona or by the "smearing" due to line-of-sight integration, especially in the IPS data. The former effect can be studied by doing autocorrelation analyses to determine the stability of both data sets. the latter effect is probably unimportant for the green line data (Musman and Altrock, 1978), but it could be critical for the IPS data, where the weighting function typically extends over 30° or more. This problem can be resolved by developing a method to invert the IPS data, giving the spatial structure of solar wind velocity. Our work in this regard is described in the next section.

Coronal magnetic field models have been provided by G. Pneumann of HAO. These models (for rotations 1601-1610) give the photospheric footprints of field lines equally spaced and assumed to be radial on a spherical surface at a height of 2.5 solar radii. From this data one can estimate the angular divergence of the field at the subscattering point of an IPS observation. Figure 3 gives scatter plots of the angular divergence versus the IPS velocity. Figure 3a shows data at all heliographic latitudes, and there is clearly no relation. In Figure 3b, which gives only velocities which map to latitudes greater than 45°N or 45°S, there is some indication of an inverse correlation. This comparison is crude, however, since what is really needed is the areal divergence of the field. Dr. Pneumann has recently provided us with additional data which will enable us to carry out a more meaningful comparison.

Interpretation of IPS Velocity Data

Inversion of the IPS velocity data to infer the spatial structure of solar wind velocity requires a knowledge of the scattering function, or turbulence profile, along the line of sight. It is known that the mean level of the turbulence varies as r^{-2}, where r is the distance from the sun (Armstrong, 1975). High speed/low speed stream interactions, however, create inhomogeneities which can cause the mean electron density to rise ten-fold or more prior to the passage of a high speed stream, and the turbulence level is likely to vary similarly. It has been argued by various authors that the turbulence level is in fact directly proportional to the mean density (e.g., Houminer, 1971). Because of our interest in the inversion problem, we have undertaken to test this hypothesis.

We test the form of the turbulence profile by calculating the IPS velocity that should be observed with an ecliptic source (3C144) given the spatial velocity distribution observed by spacecraft. The spacecraft data was obtained from the earth orbiting IMP satellites and covers the years 1973-early 1976. These spacecraft measured proton densities as well as velocities. We predict the IPS velocity by integrating along the line of sight using weak scattering theory with a power law turbulence spectrum of index 2.7, which is typical for the portion of the spectrum responsible for IPS (Harmon, 1975). The structure of the medium is assumed to be stationary over the time necessary for a solar wind stream to corotate from the scattering region to the earth, typically a few days. This is a good assumption for the time period in question, since prominent features often persisted for several rotations. By varying the turbulence profile until the predicted IPS velocities match the observed velocities, we can choose a "best" profile.

A typical sequence of solar wind streams is shown in Figure 4. Here the turbulence profile is proportional to the density. It will be noted that the simulated and observed IPS velocities are poorly matched. By contrast, the turbulence profile of Figure 5 gives a much better match. Figure 5 illustrates the two dominant features that characterize the "best fit" profiles for a large body of 1973-1975 data: 1) The turbulence enhancement lags the density enhancement by about a day, so that it lies within the body of the high velocity stream, and 2) in wide, flat streams, enhanced turbulence extends well inside the stream body, into regions where the density is often in rarefaction. Even a constant profile (i.e., no enhancements) gives a better match than a profile which is proportional to the density, but it too is inferior to the sort of profile shown in Figure 5. This result has implications for solar wind turbulence theory as for the interpretation of IPS data. A paper describing this work in detail is underway.

This work is the first step in the development of a velocity inversion method. We next intend to examine the turbulence profile of the higher latitude solar wind, where stream/stream interactions are weaker. With a global model of the turbulence profile, it will be possible to infer the spatial structure of velocity from a continuous time series of IPS observations and subsequently to make more meaningful comparisons with coronal data.

Figure Captions

Figure 1: Geometry of an IPS observation.

Figure 2: Scatter plot of IPS velocity versus coronal 5303 Å intensity for rotations 1630-1640. Different symbols denote different radio sources.

Figure 3: Scatter plots of IPS velocity versus angular divergence of the coronal magnetic field for rotations 1601-1610. a. all data; b. data mapping to latitudes greater than 45°S or 45°N. Different symbols denote different sources.

Figure 4: IPS velocities predicted from spacecraft data and actual IPS measurements. Plots, from top, are 1) spacecraft velocity, 2) turbulence profile (here identical to the density profile), 3) density profile, 4) observed IPS midpoint velocities (crosses) with simulated data, 5) observed IPS peak velocities (crosses) with simulated data. The time period is day 195 to day 225 of 1974.

Figure 5: Same as Figure 4, but with a different turbulence profile.

References

Armstrong, J.W., Ph.D. Thesis, University of California, San Diego, 1975.

Coles, W. A., and J. J. Kaufman, Radio Science, in press, 1978.

Coles, W. A. and B. J. Rickett, J. Geophys. Res. 81, 4797, 1976.

Coles, W. A., B. J. Rickett, and V. H. Rumsey, in Solar Wind Three: Proceedings of the Asilomar Solar Wind Conference, Univ. of Calif., Los Angeles, Inst. of Geophys. and Planet. Phys., p. 351, 1974.

Dennison, P. A. and A. Hewish, Nature, 213, 343, 1967.

Fisher, R. R., and S. A. Musman, Astrophys. J., 195, 801, 1975.

Harmon, J. K., Ph.D. Thesis, University of California, San Diego, 1975.

Houminer, Z., Nature Phys. Sci., 231, 165, 1971.

Kaufman, J. J., Ph.D. Thesis, University of California, San Diego, 1976.

Krieger, A. J., A. F. Timothy, and E. C. Roelof, Solar Phys., 29, 505, 1973.

Levine, R. H., M. D. Altschuler, and J. W. Harvey, J. Geophys. Res., 82, 1061, 1977.

Musman, S. A., and R. C. Altrock, J. Geophys. Res., (in press) 1978.

Rickett, B. J., D. G. Sime, N. R. Sheeley, W. R. Crockett, and R. Tousey, J. Geophys. Res., 81, 3845, 1976.

Sime, D. G., Ph.D. Thesis, University of California, San Diego, 1976.

Snyder, C. W., M. Neugebauer, and U. R. Rao, J. Geophys. Res., 68, 6361, 1963.

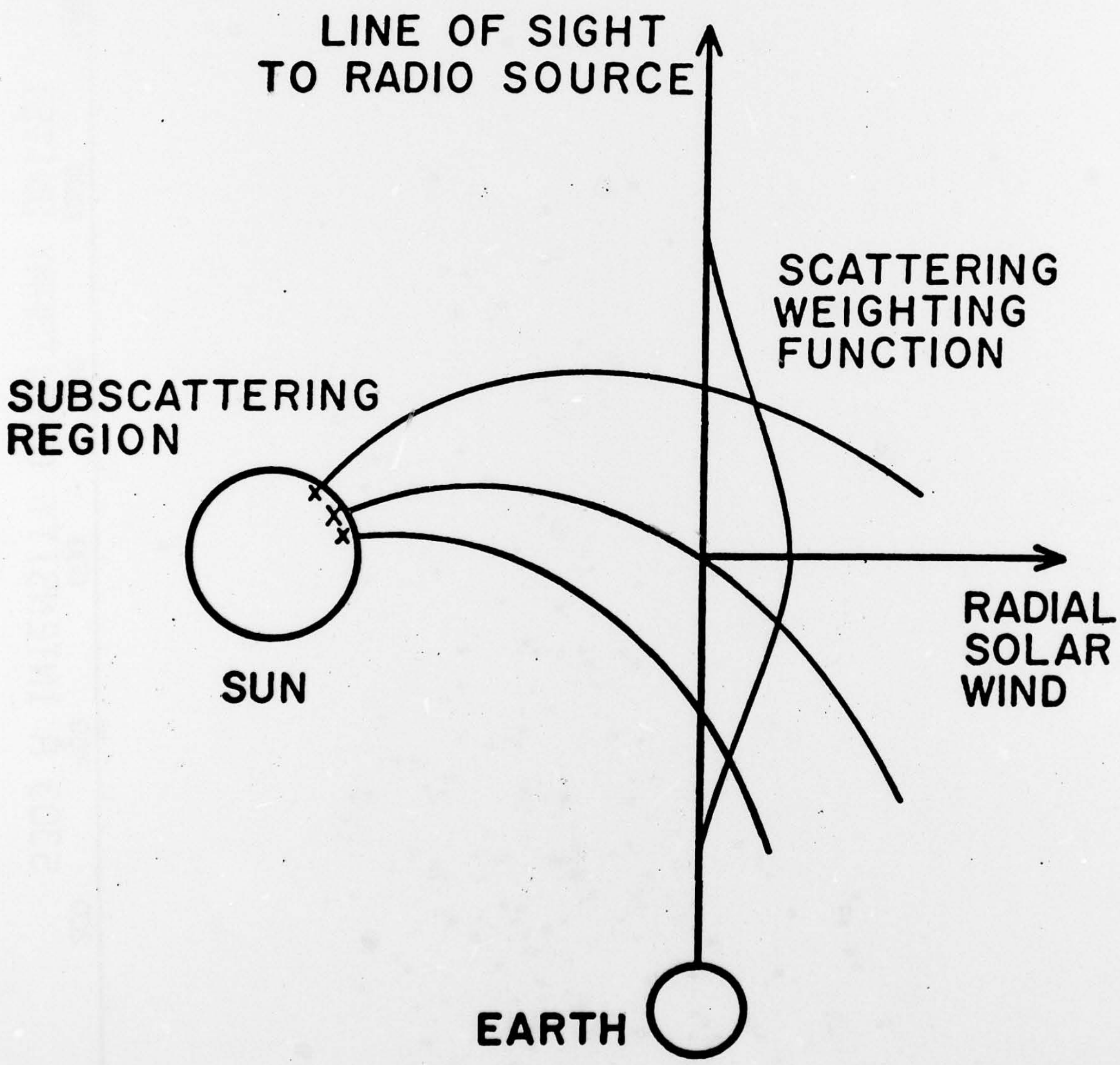
LINE OF SIGHT
TO RADIO SOURCE
SCATTERING
WEIGHTING
FUNCTION
SUBSCATTERING
REGION
SUN
RADIAL
SOLAR
WIND
EARTH

Figure 1

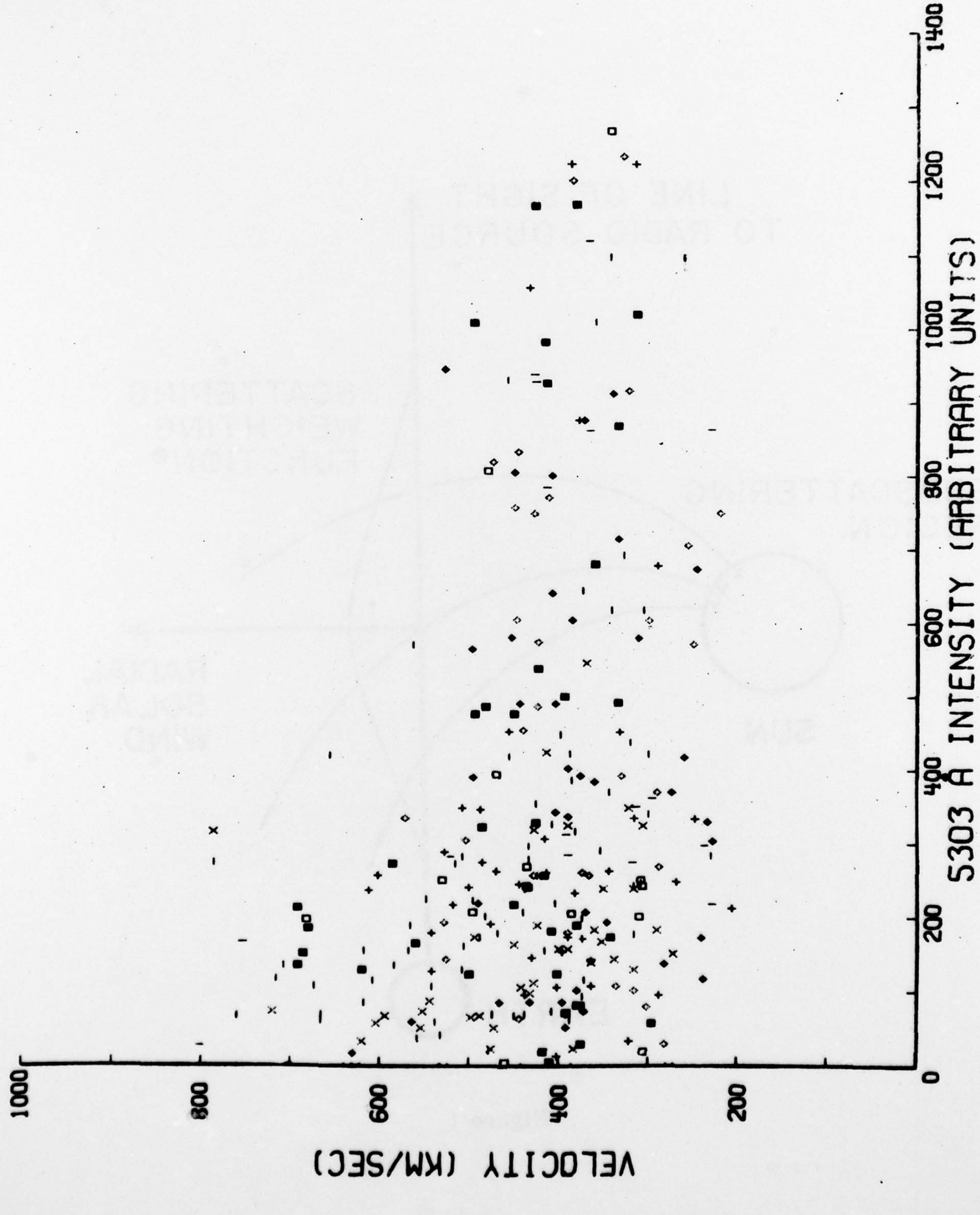
VELOCITY (KM/SEC)
1000
800
600
400
200
0
200
400
600
800
1000
1200
1400
5303 Å INTENSITY (ARBITRARY UNITS)

Figure 2

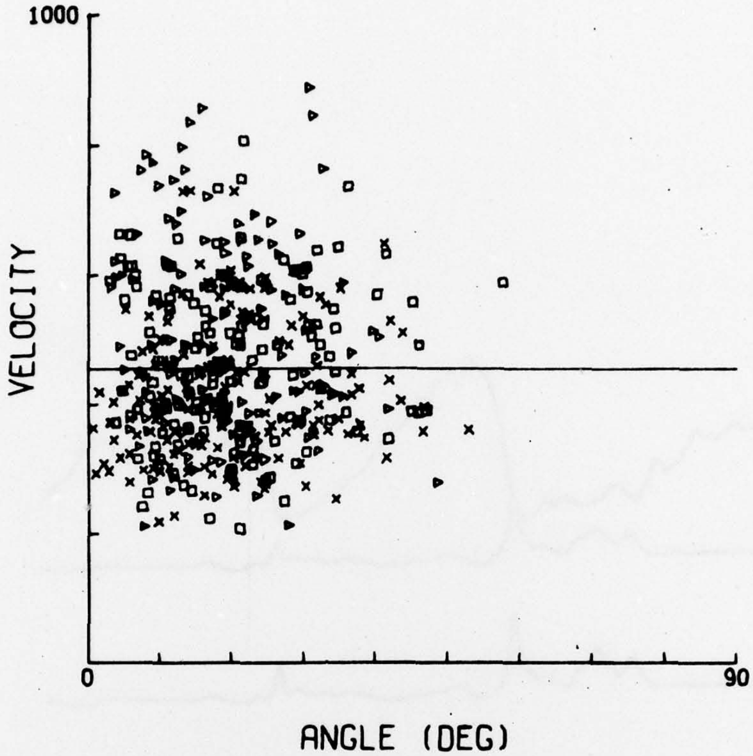

a

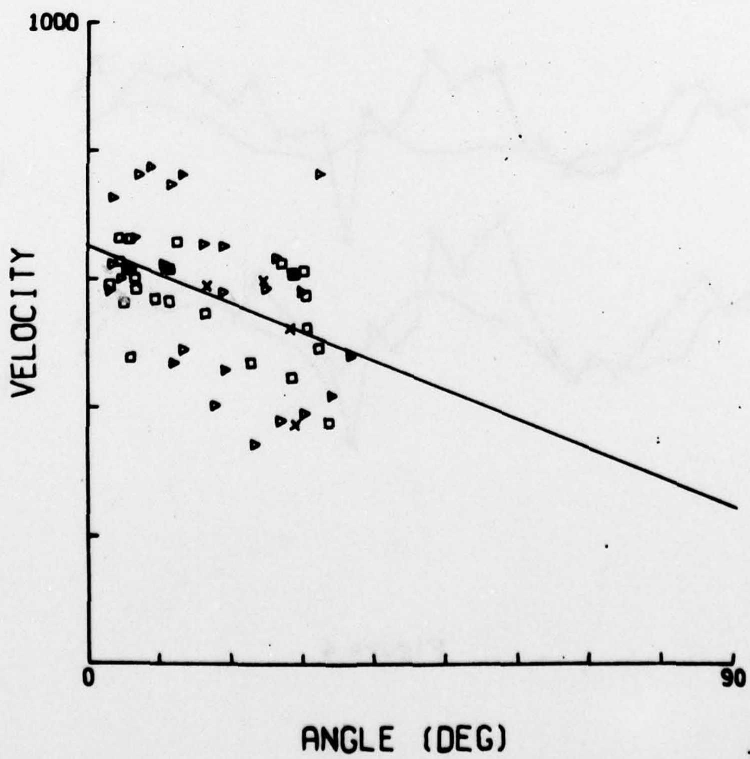

b

Figure 3

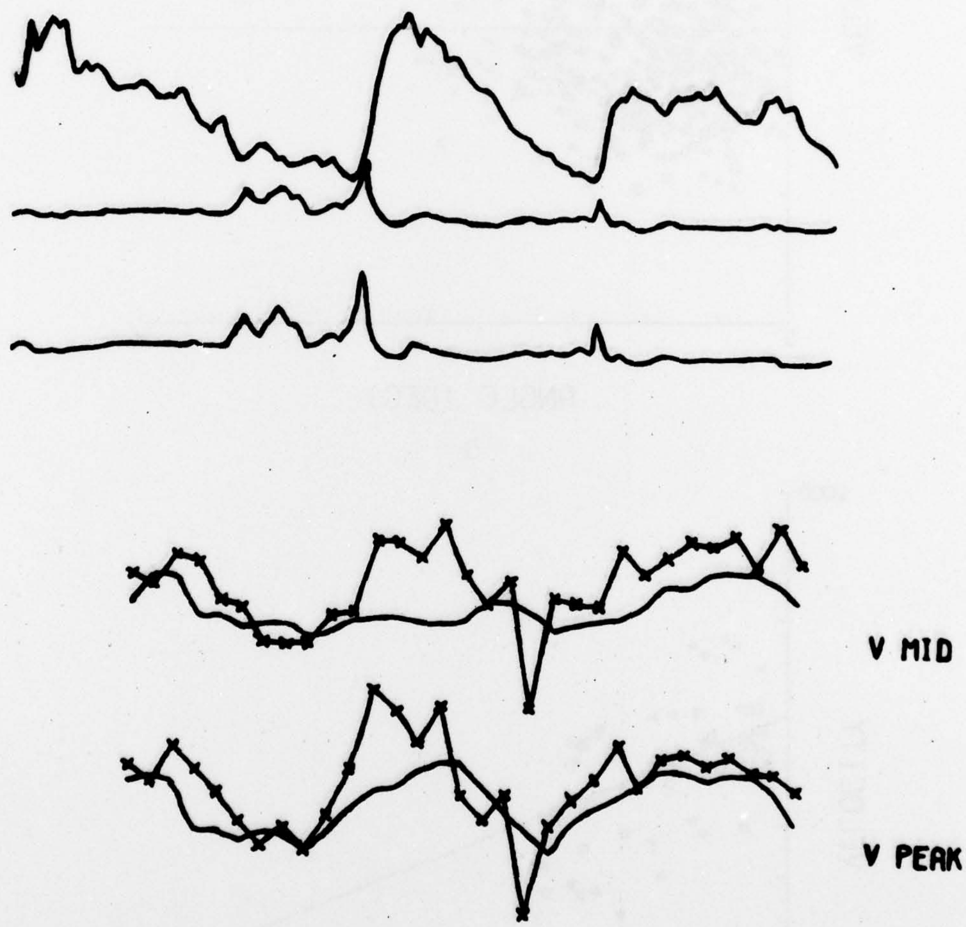

Figure 4

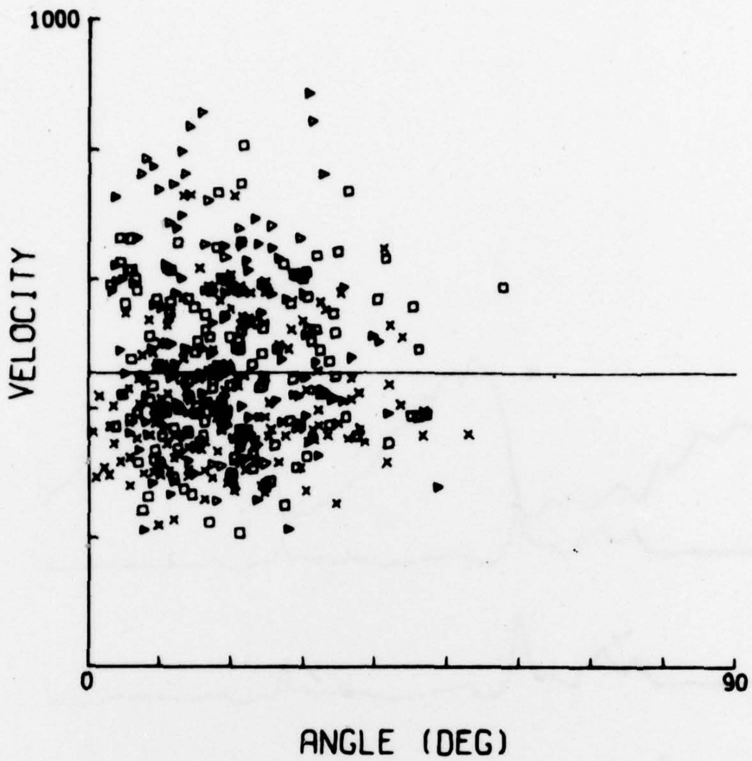

a

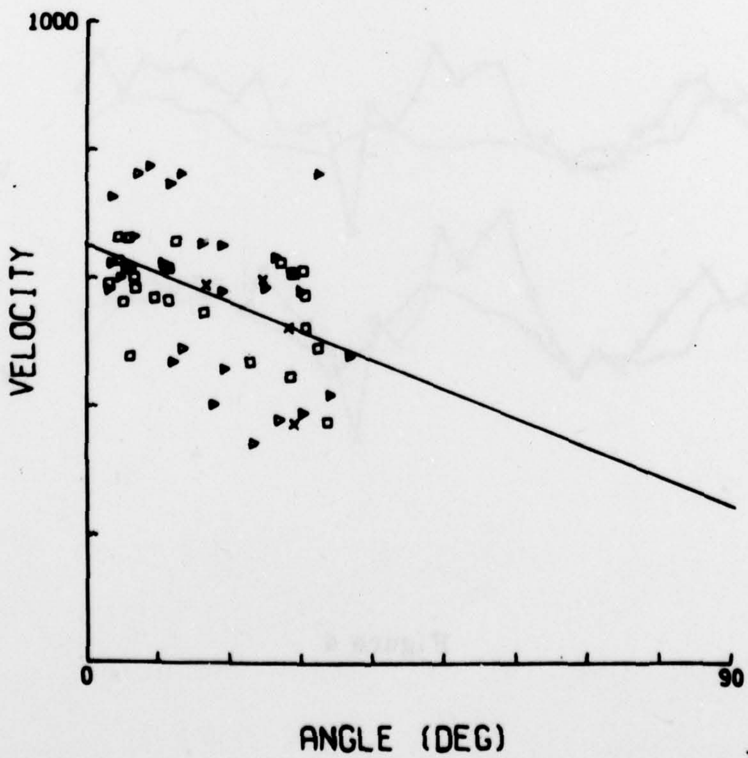

b

Figure 3

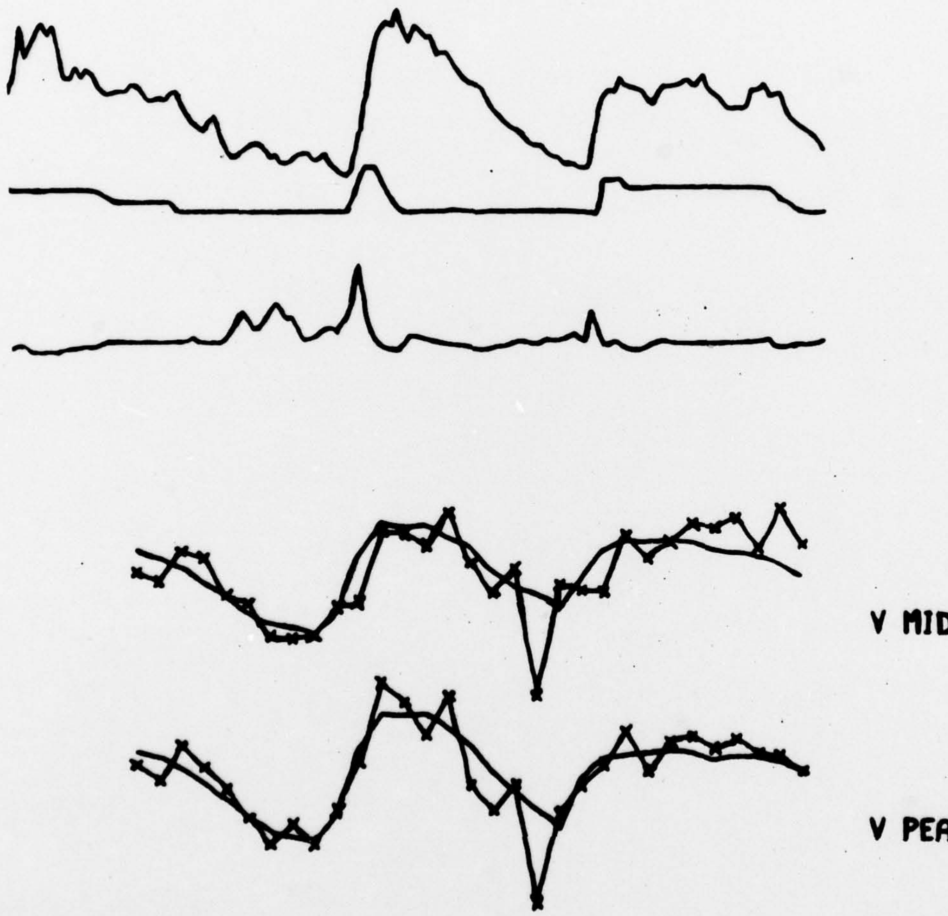

Figure 5